Available online at www.sciencedirect.com

ScienceDirect

Materials Today: Proceedings 5 (2018) 9804–9810

materialstoday: PROCEEDINGS

www.materialstoday.com/proceedings

IC-FNM 2016

Transport Properties of Calcium Doped $YMnO_3$ Thin Film

K.N. Rathod[a], Keval Gadani[a], Zalak Joshi[a], Davit Dhruv[a], A.D. joshi[b], K. Asokan[c], P.S. Solanki[a] and N.A. Shah[a,*]

[a]*Department of Physics, Saurashtra University, Rajkot – 360005, India*
[b]*Department of Nanoscience and Advanced Materials, Saurashtra University, Rajkot – 360005, India*
[c]*Inter University Accelerator Centre, Aruna Asaf Ali Marg, New Delhi – 110067, India*

Abstract

$YMnO_3$ thin film, doped with Ca at Y–site, was grown on n–type single crystalline Si substrate using pulsed laser deposition (PLD) technique. The structural measurement using X–ray diffraction (XRD) shows single phasic hexagonal unit cell structure. From d–spacing, calculated lattice strain is observed to be compressive in nature. Atomic force microscopy (AFM) was employed to study morphology of the film surface. The current–voltage characteristic exhibits a strong dependence on temperature. Space charge limited conduction (SCLC) mechanism has been best fitted to I–V results owing to the important role of trap centers. An efficient normal to backward diode behavior transition has been observed with increase in temperature.

Selection and/or Peer-review under responsibility of International Conference on Functional Nano-Materials, 2016.

Keywords: Manganite; Manganite; Transport; $YMnO_3$; Thin film; Backward diode.

1. Introduction

Most intense research is going on for manganites in recent years owing to the discovery of colossal magnetoresistance (CMR). CMR manganites exhibit interrelated structural and physical properties which allow them to be used as magnetic memory storage and read–write devices. Strong correlation between transport, magnetic and magnetotransport properties is one of the most elementary properties of manganites [1–3]. Intervened role of oxygen between Mn^{3+} and Mn^{4+} produces Zener double exchange (ZDE) which in turn results into the transition

* Corresponding author. Tel.: +91-281-258-8428; fax: +91-281-258-6983.
E-mail address: snikesh@yahoo.com

Selection and/or Peer-review under responsibility of International Conference on Functional Nano-Materials, 2016.

from insulating to metallic and paramagnetic to ferromagnetic manganite [4]. Ordering of Mn spins suppresses the scattering of charge carriers causing decrease in resistivity transition temperatures [5].

$YMnO_3$ (YMO) based manganites with ABO_3 type perovskite structure have been extensively studied in recent years [6,7]. YMO displays, both, hexagonal and orthorhombic phases depending on heat treatment provided to the material [8]. YMO shows ferroelectricity arising from its geometry and static–electric effect [9]. Hexagonal YMO materials are ideal to be used as non–volatile for memory devices because of having stable intrinsic charged domain walls [10].

Epitaxial strain introduced by the growth of ABO_3 type perovskite on single crystalline substrate induces variations in bond length and angles resulting into the change in its properties. Hole doped perovskites are known to possess strain effects [11]. Recently, Dhruv et al [6,7] have reported compressive strain, induced in hole doped YMO thin films. Basically, strain plays an important role in governing the charge transport in mixed valent manganites [12–14]. Dhruv et al [6] have grown polycrystalline films of doped YMO manganites and finally annealed them at two different temperatures. Both the films show a variation in lattice strain and hence a strong effect on transport, device characteristics and electroresistance (ER) behavior. They have also investigated the role of strain in governing the capacitive nature of the manganite–substrate interface [7].

By keeping in mind all above aspects, we have fabricated hole (Ca^{2+}) doped YMO film on n–type single crystalline Si substrate. In this communication, we have studied structural, morphology and transport properties of Ca^{2+} doped YMO/Si films. Device characteristics of the presently studied film have been understood in terms of space charge limited conduction (SCLC) mechanism and backward diode characteristics.

2. Experimental Details

Preparation of Ca–doped $YMnO_3$ ($Y_{0.95}Ca_{0.05}MnO_3$: YCMO) thin film was carried out by sophisticated pulsed laser deposition (PLD) technique using KrF excimer laser. YCMO thin film with thickness ~ 300nm was deposited on n–type Si substrate having *(001)* orientation. Parameters used for the fabrication of thin films are: laser energy = 1.8J/cm^2, frequency = 10Hz, substrate temperature = 800^{o}C, oxygen partial pressure = 10^{-5} Torr. Thin film was then followed by the calcinations at 300^{o}C and annealing at 700^{o}C for 30 minutes and 24 hours, respectively. For structural and microstructural studies, XRD and AFM measurements were carried out. In present case, two probe method was used to performed transport mechanisms.

3. Results and Discussion

3.1. Structural Studies

Figure 1 (a) shows XRD pattern of YCMO/Si film reveals the high purity of the film with no additional peak corresponding to the impurity or secondary phase, observed in the pattern. Peak indexing of YCMO shows hexagonal unit cell structure. YCMO film, as shown in figure 1 (a), is grown in the parallel orientation with that of the Si substrate. Though, the observed *(111)* peak at ~ 29^o confirms that YCMO film is grown with polycrystalline nature. Figure 1 (b) shows an enlarged view of separated *(100)* peak of YCMO and Si substrate which shows a clear separation between the film and substrate peaks indicating a presence of lattice mismatch between them and signifies an existence of structural strain between the polycrystalline hexagonal YCMO film lattice and single crystalline Si substrate. The strain originated in structure at the interface can be quantified as: δ (%) = $[(d_{substrate} - d_{film}) / d_{substrate}] \times 100$. Positive value of δ corresponds to tensile strain while negative value indicates the presence of compressive strain. Calculated lattice strain is found to be ~ –1.53 which implies a presence of compressive strain between the film and substrate lattices.

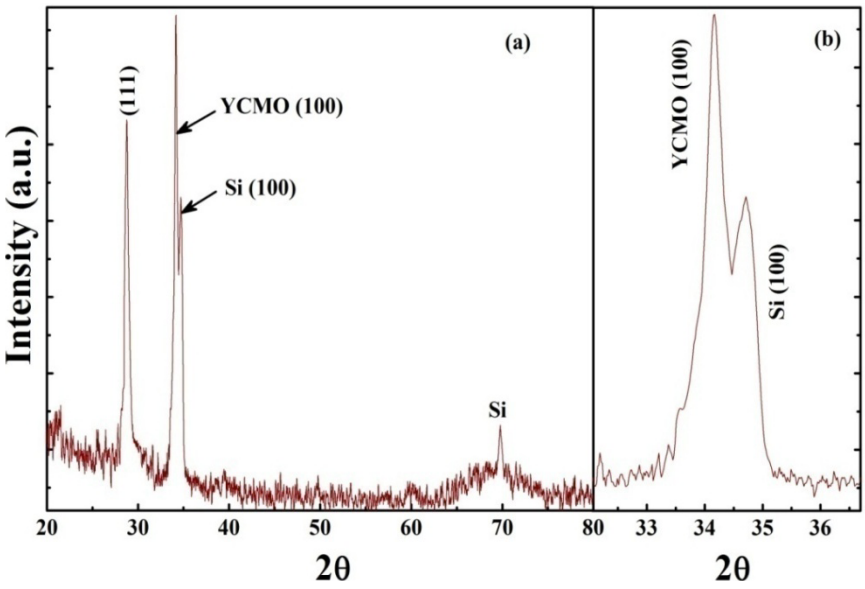

Fig. 1. XRD pattern of (a) YCMO/Si thin film; (b) an enlarged view of *(100)* peaks.

3.2. Surface Morphology

In the inset figure 2, 2D AFM micrograph is shown which illustrates small crystalline grains. Surface roughness histogram (figure 2) shows maximum 137nm height and average surface roughness is ~ 40nm of the film understudy. Higher surface roughness of proposed YCMO/Si thin film can be correlated with the island like grain growth observed in the 2D micrograph of AFM (inset of figure 2). We have also checked the surface roughness of bare Si substrate (purchased from the Crystal GmbH, Germany), prior to perform the PLD experiment for fabrication of film, and it is found that the substrate surface possesses roughness < 0.5nm which is much smaller than that of the YCMO film.

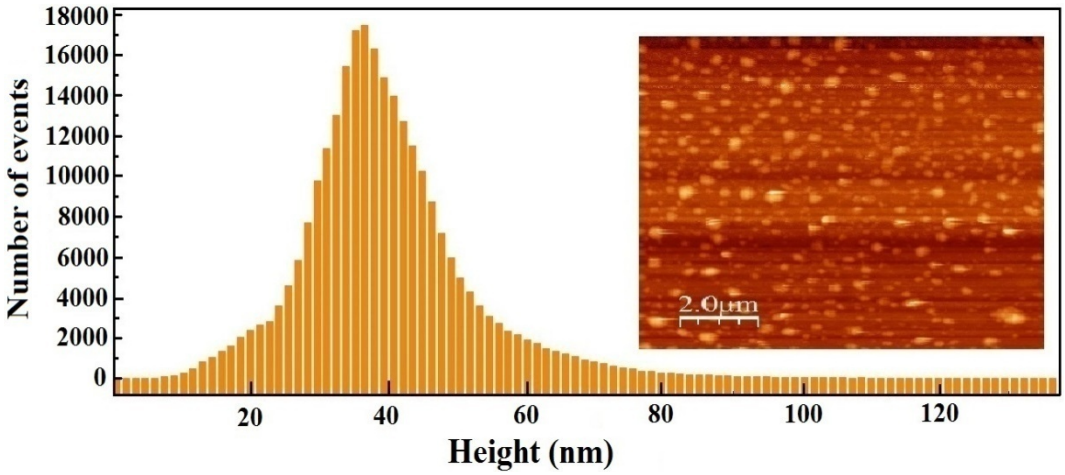

Fig. 2. AFM surface roughness histogram with 2D AFM micrograph.

3.3. Transport Properties

Current–voltage characteristics, recorded at various temperatures ranging from 100 to 300K with sweeping of voltages from (–5V) to (+5V), are shown in figure 3. Inset of figure 3 shows a schematic diagram of YCMO/Si device in which YCMO film acts as p–type where as substrate Si as n–type. Current perpendicular to the plane (CPP) mode was used to perform current–voltage measurements. Silver paste was used as electrodes to provide ohmic contact, since there is a fair similarity between the work functions of Ag (~ 4.7eV [15]) and presently studied YCMO (~ 4.63±x; where x is the comparatively small number) (based on the reported value of pure hexagonal $YMnO_3$ compound ~ 4.63eV [16]). Current is in the range of nA for all the temperatures which shows large resistance of the thin film understudy. With application of voltage, current increases which indicate that charge carriers get enough energy to cross the interfacial barrier formed between YCMO film and Si substrate. Sudden rise of current is observed at saturation voltage (V_S) which signifies small resistance above saturation voltage. Effective charge carrier density increases with temperature [17] resulting in the improved conduction at higher temperatures due to which saturation voltage also reduced with increase in temperature. In addition, at higher temperatures, the current in forward direction is very small as compared to reverse while at lower temperatures, forward current is larger as compared to reverse bias condition which implies backward diode like behavior at higher temperatures.

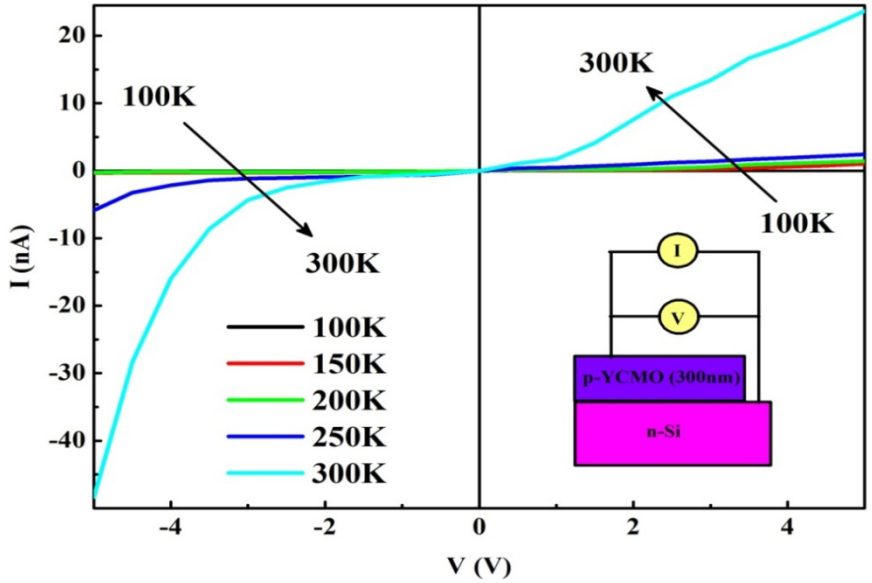

Fig. 3. Typical I–V characteristics measured at temperatures ranging from 100 to 300K; Inset: Schematic illustration of manganite based device junction with CPP mode geometry.

As a function of voltage, square root current has been plotted and linearly fitted, as shown in figure 4. Fits in figure 4 suggest a significant dominant role of injected carriers over thermally generated carriers. Straight line fitting of the plot $I^{1/2}$ vs. V signifies the presence of space charge limited conduction (SCLC) mechanism in YCMO/Si film/interface. Space charge conduction is generally present when the trapping centres are available, due to which role of trapping centres becomes important. In present case, Si has been used as a substrate which is well known to have trap centres [18]. These trap centres in Si substrate may arise due to defects, impurities, dangling bonds, etc. These centres trap the charge carriers and show reduced charge carriers flow but after particular voltage, called trap free voltage, these trapped charge carriers become free to flow across the interface region. With increase in temperature from 100 to 300K, the values of slope obtained from fittings (figure 4) increases which indicates that the ratio between free to trapped charge carriers get increased. Large number of free charge carriers at higher temperatures is due to the thermal process allowing higher conduction in the film.

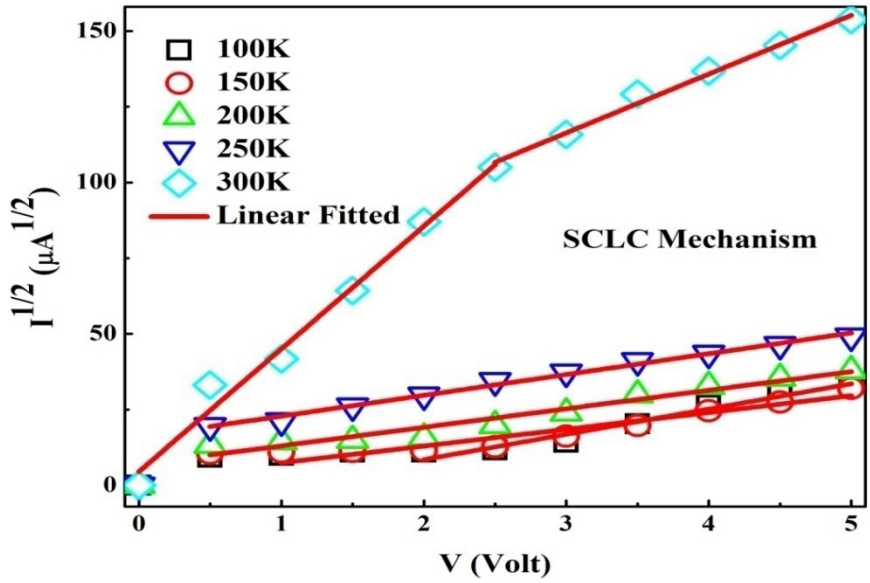

Fig. 4. Straight line fitted square root current as a function of voltage ($I^{1/2}$–V) plots showing SCLC mechanism.

Temperatures ranging from 100 to 200K show normal diode like behavior while temperatures between 250 and 300K show backward diode like behavior. There are few reports available for the observation of backward diode like behavior [19–21]. It is reported that Si based device demonstrates backward diode behavior [22]. Backward diodes are generally used as a small signal linear detector.

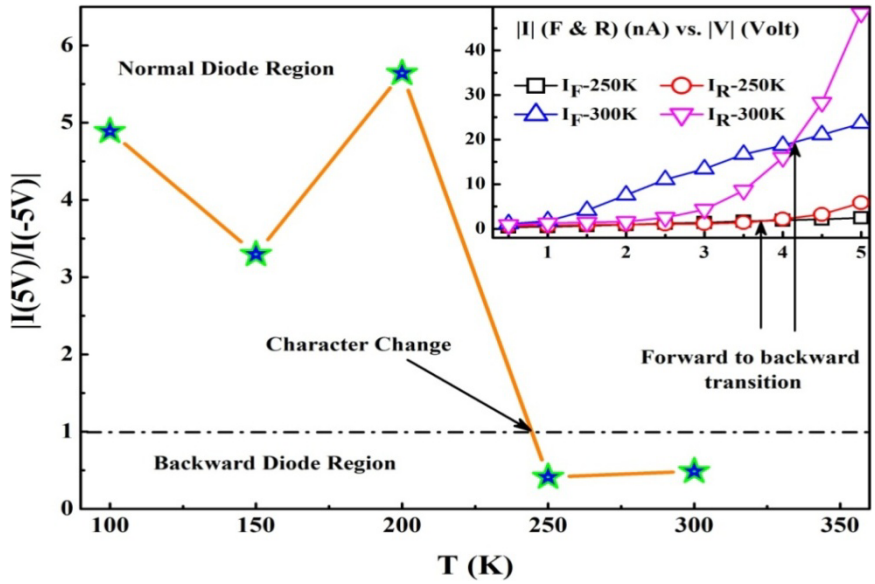

Fig. 5. Normal to backward behavior with respect to temperature; Inset: |I|–|V| plots to confirm backward behavior in 250 and 300K temperatures.

To verify the presence of backward diode like characteristics observed in the I–V characteristics in figure 3, we have plotted |I(5V)|/|I(–5V)| ratio at different temperatures in figure 5. At lower temperatures, well below 250K, |I(5V)|/|I(–5V)| >1 which signifies the normal diode like behavior while at higher temperatures, ≥ 250K, the ratio is found to be less than 1. This suggests that the presently studied YCMO/Si film shows normal diode like character which gets transformed to backward diode character at higher temperatures. Inset of figure 5 shows the positive

voltage dependent |I| for, both, forward and reverse biasings. This suggests that, at higher temperatures (≥ 250K), character transition from normal to backward is also influenced by an applied voltage. As shown in the inset of figure 5, at lower applied voltages (for 250 & 300K), film exhibits normal diode behavior which gets transformed to backward diode behavior. With increase in temperature from 250 to 300K, the transforming voltage (required to transform the behavior from normal to backward) shifts towards higher value (from 3.7 to 4.1V). Presently observed backward diode character change aspect of YCMO/Si film can be understood in terms of leakage current effect. If the leakage current in reverse bias mode is found to be larger than the forward one, the device shows a backward diode like characteristics [11]. Influence of temperature and applied transforming voltage suggests the modifications in the leakage current due to temperature and electric field [11].

4. Conclusion

In summary, Ca doped $YMnO_3$ thin film (~ 300nm thickness) on single crystalline (100) Si substrate was successfully prepared using pulsed laser deposition (PLD) technique. Structural analysis revealed single phasic hexagonal structure with negative lattice mismatch between YCMO film and Si substrate implying compressive strain. Surface roughness show higher roughness of thin film understudy. Transport studies confirming temperature dependent variation in current, resulted from effective charge carrier density change with voltage and temperature. Si substrate assisted trap centre signifies space charge limited conduction. Transition from normal to backward behavior is observed at higher temperatures and higher applied voltage which has been correlated with possibility of large reverse biased leakage current across the YCMO/Si interface.

Acknowledgement

Author KNR is thankful to UGC, New Delhi for financial support in the form of UGC (BSR) Meritorious Fellowship [File No.: F.25-1/2014-15(BSR)/7-156/2007(BSR)]. Author ZJ is thankful to UGC, New Delhi for financial support in the form of UGC (BSR) Meritorious Fellowship [File No.: F.25-1/2013-14(BSR)/7-156/2007(BSR)]. Author KG is thankful to Inter University Accelerator Centre, New Delhi for financial assistance in the form of junior research fellowship [File No.: BTR 57309]. Authors are thankful to Dr. Indra Sulania, IUAC, New Delhi for providing AFM facility.

References

[1] S.B. Kansara, D. Dhruv, B. Kataria, C.M. Thaker, S. Rayaprol, C.L. Prajapat, M.R. Singh, P.S. Solanki, D.G. Kuberkar, N.A. Shah, Ceram. Int. 41 (2015) 7162–7173.
[2] S.B. Kansara, D. Dhruv, Z. Joshi, D.D. Pandya, S. Rayaprol, P.S. Solanki, D.G. Kuberkar, N.A. Shah, Appl. Surf. Sci. 356 (2015) 1272–1281.
[3] A. Krichene, P.S. Solanki, D. Venkateshwarlu, S. Rayaprol, V. Ganesan, W. Boujelben, D.G. Kuberkar, J. Magn. Magn. Mater. 381 (2015) 470–477.
[4] J.H. Markna, R.N. Parmar, D.G. Kuberkar, R. Kumar, D.S. Rana, S.K. Malik, Appl. Phys. Lett. 88 (2006) 152503:1–3.
[5] P.S. Solanki, R.R. Doshi, U.D. Khachar, M.V. Vagadia, A.B. Ravalia, D.G. Kuberkar, N.A. Shah, J. Mater. Res. 25 (2010) 1799–1802.
[6] D. Dhruv, Z. Joshi, S.B. Kansara, D.D. Pandya, J.H. Markna, K. Asokan, P.S. Solanki, D.G. Kuberkar, N.A. Shah, Mater. Res. Exp. 3 (2016) 036402:1–9.
[7] D. Dhruv, Z. Joshi, S.B. Kansara, M.J. Keshvani, D.D. Pandya, K. Asokan, P.S. Solanki, D.G. Kuberkar, N.A. Shah, Adv. Sci. Lett 22 (2016) 843–848.
[8] J. Park, J.G. Park, G.S. Jeon, H.Y. Choi, C. Lee, W. Jo, R. Bewley, K.A. McEwen, T.G. Perring, Phys. Rev. B 68 (2003) 104426:1–6.
[9] B.V. Aken, T. Palstra, A. Filippetti, N. Spaldin, Nat. Mater. 3 (2004) 164–170.
[10] P. Gao, C.T. Nelson, J.R. Jokisaari, Y. Zhang, S.H. Baek, C.W. Bark, E. Wang, Y.M. Liu, J.Y. Li, C.B. Eom, X.Q. Pan, Adv. Mater. 24 (2012) 1106–1110.
[11] K. Gadani, D. Dhruv, Z. Joshi, H. Boricha, K.N. Rathod, M.J. Keshvani, N.A. Shah, P.S. Solanki, Phys. Chem. Chem. Phys. 18 (2016) 17740–17749.
[12] P.S. Solanki, R.R. Doshi, U.D. Khachar, R.J. Choudhary, D.G. Kuberkar, Mater. Res. Bull. 46 (2011) 1118–1123.
[13] R.N. Parmar, J.H. Markna, P.S. Solanki, R.R. Doshi, P.S. Vachhani, D.G. Kuberkar, J. Nanosci. Nanotechnol. 8 (2008) 4146–4151.
[14] P.S. Solanki, R.R. Doshi, U.D. Khachar, D.G. Kuberkar, Physica B 406 (2011) 1466–1470.
[15] C.Y. Chang, T.P. Juan, J.Y. Lee, Appl. Phys. Lett. 88 (2006) 072917:1–3.
[16] H. Han, S. Song, J.H. Lee, K.J. Kim, G.W. Kim, T. Park, H.M. Jang, Chem. Mater. 27 (2015) 7425–7432.
[17] P. Miao, Y. Zhao, N. Luo, D. Zhao, A. Chen, Z. Sun, M. Guo, M. Zhu, H. Zhang, Q. Li, Sci. Rep. 6 (2016) 19965:1–9.
[18] W.L. Kalb, S. Haas, C. Krellner, T. Mathis, B. Batlogg, Phys. Rev. B 81 (2010) 155315:1–13.

[19] Z.G. Sheng, Y.P. Sun, X.B. Zhu, J.M. Dai, W.H. Song, Z.R. Yang, L. Hu, R.R. Zhang, J. Phys. D: Appl. Phys. 41 (2008) 135008:1–6.
[20] Y.W. Xie, J.R. Sun, D.F. Guo, B.G. Shen, X.Y. Zhang, Europhys. Lett. 87 (2009) 57006:1–5.
[21] Y. Cui, L. Zhang, R. Wang, G. Xie, Thin Solid Films 516 (2008) 2292–2295.
[22] N. Jin, R. Yu, S.Y. Chung, P.R. Berger, P.E. Thompson, P. Fay, IEEE Electron Device Lett. 26 (2005) 575–578.